On the Analogy of B−BO and B−Au Chemical Bonding in $B_{11}O^-$ and $B_{10}Au^-$ Clusters

Hua-Jin Zhai,[†] Chang-Qing Miao,[‡] Si-Dian Li,*[,‡] and Lai-Sheng Wang*[,†]

Institute of Molecular Sciences, Shanxi University, Taiyuan 030006, People's Republic of China, Institute of Materials Science and Department of Chemistry, Xinzhou Teachers' University, Xinzhou 034000, Shanxi, People's Republic of China, and Department of Chemistry, Brown University, Providence, Rhode Island 02912, United States

Received: September 11, 2010; Revised Manuscript Received: October 15, 2010

During photoelectron spectroscopy experiments, the spectra of $B_{11}O^-$ and $B_{10}Au^-$ clusters are found to exhibit similar patterns except for a systematic spectral shift of ~0.5 eV, hinting that they possess similar geometric structures. The electron affinities are measured to be 4.02 ± 0.04 eV for $B_{11}O$ and 3.55 ± 0.02 eV for $B_{10}Au$. DFT calculations at the B3LYP level show that $B_{11}O^-$ and $B_{10}Au^-$ adopt similar C_1 (^1A) ground states, which are based on the quasiplanar B_{10} cluster interacting with a BO unit and Au, respectively. The $B_{11}O^-$ and $B_{10}Au^-$ clusters are thus valent isoelectronic because both BO and Au can be viewed as monovalent units, forming highly covalent B−BO and B−Au bonds analogous to the B−H bond in $B_{10}H^-$. For $B_{10}Au^-$, we also find a highly symmetric D_{10h} ($^1A_{1g}$) planar molecular wheel as a minimum on the potential energy surface. However, it is 45 kcal/mol above the ground state at the B3LYP level and not viable for experimental observation. Natural bond orbital analyses reveal interesting *covalent* versus *ionic* B−Au bonding in the C_1 $B_{10}Au^-$ and D_{10h} $B_{10}Au^-$ structures, respectively, providing insight for the design of D_{nh} MB_n molecular wheels.

1. Introduction

Boron possesses interesting chemical bonding properties and has played essential roles in advancing chemical bonding models.[1,2] Primarily due to the electron deficiency of boron, delocalized three-center two-electron bonds are common in boranes[3] and elemental boron clusters.[4−8] Boron also forms interesting oxides, and the simplest diatomic BO molecule (boronyl) has long been recognized as a σ-radical[9−11] with a B≡O triple bond. BO and BO^- are valent isoelectronic to CN and CN^-/CO, respectively, which are important inorganic ligands. However, despite decades of persistent interest in boron oxides,[12,13] boronyl chemistry remains relatively unknown.[14−20]

We are interested in elucidating the electronic structure and chemical bonding of boron oxide clusters using photoelectron spectroscopy (PES) and theoretical calculations.[11,21−23] We recently characterized two boron oxide clusters,[22] $B_3O_2^-$ and $B_4O_3^-$, which possess linear $B(BO)_2^-$ ($D_{\infty h}$, $^3\Sigma_g$) and triangular $B(BO)_3^-$ (D_{3h}, $^2A_2''$) structures, that is, two and three boronyls bonded to a single B atom. We further showed that the $B_4O_2^{2-}$ cluster has a linear diboronyl diborene ground state, $B_2(BO)_2^{2-}$, which can be viewed as two boronyls bonded to a B_2 core and concurrently features a rare B≡B triple bond.[23] Our combined experimental and theoretical studies[21−23] have stimulated further theoretical efforts on boron oxide clusters.[24−27] However, none of the $B_m(BO)_n^-$ ($m > 2$) clusters has been characterized experimentally. Among earlier studies relevant to boronyl chemistry, gas-phase microwave[14] and matrix infrared spectroscopy[15] suggested rather strong B−O linkage in XBO. PES data revealed a similarity between H_3CBO and its isoelectronic H_3CCN,[16] and thus the B−O linkage in the former was described as a triple bond. Very recently, the first metal boronyl compound featuring a B≡O triple bond was synthesized in the bulk.[18]

The bonding properties of Au in alloy clusters represent yet another interesting aspect in cluster research.[28−30] The isolobal analogy between a gold phosphine unit and a hydrogen atom has helped the rationalization of the structure and bonding in Au compounds.[28] Further analogy between a bare Au atom and H has been discovered recently in gas-phase binary Au clusters.[31−35] In systematic studies on Si−Au clusters, $SiAu_4$, $SiAu_n$ ($n = 2, 3$), Si_2Au_n ($n = 2, 4$), and Si_3Au_3 were shown to possess structures and bonding similar to the silane SiH_4, SiH_n, Si_2H_n ($n = 2, 4$), and Si_3H_3, respectively.[31−33] For the $B_7Au_2^-$ alloy cluster,[34] the B−Au bonding was shown to be covalent, similar to the B−H bonding in $B_7H_2^-$.[36] The $B_{10}Au^-$ cluster in the current work serves as another example to further test the Au/H analogy in Au alloy clusters. Moreover, stimulated by the elucidation of the chemical bonding in planar boron clusters,[5−7] there is increasing computational interest in planar MB_n molecular wheels.[37−44] Among these MB_n clusters are the D_{10h} $B_{10}Au^-$ anion[39] and its valent isoelectronic D_{10h} $B_{10}Cu^-$ and D_{10h} $B_{10}Zn$ species.[40] However, the viability of all these D_{10h} molecular wheels has yet to be confirmed experimentally.

Here we report a combined PES and theoretical study of $B_{11}O^-$ and $B_{10}Au^-$ clusters. During PES experiments on boron oxide clusters and B−Au alloy clusters, $B_{11}O^-$ and $B_{10}Au^-$ are observed to exhibit similar PES patterns except for a slight shift in binding energies. Theoretical calculations show that $B_{11}O^-$ and $B_{10}Au^-$ possess similar C_1 (^1A) ground-state structures, where the $B_{11}O^-$ cluster can be described as $B_{10}(BO)^-$, that is, a boronyl B≡O unit interacting with an aromatic B_{10}^- core. Both the B−BO and B−Au bonds are shown to be highly covalent, analogous to the B−H bond. The current study highlights not only the robustness of the B≡O boronyl group in boron-rich boron oxide clusters but also the Au/H analogy in B−Au complexes. A highly symmetric D_{10h} $B_{10}Au^-$ molec-

* To whom correspondence should be addressed. E-mail: lisidian@yahoo.com (S.-D.L.); Lai-Sheng_Wang@brown.edu (L.-S.W.).
† Brown University.
‡ Shanxi University and Xinzhou Teachers' University.

10.1021/jp108668t
Published on Web 10/29/2010

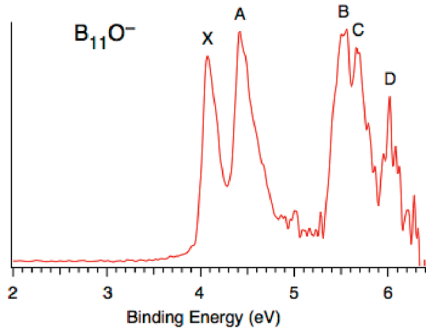

Figure 1. Photoelectron spectrum of $B_{11}O^-$ at 193 nm (6.424 eV).

ular wheel is shown to be a high-lying minimum 45 kcal/mol above the C_1 ground state. The bonding of this cluster is compared with that of the C_1 global minimum, providing insight into the stability of D_{nh}-type MB_n molecular wheels.

2. Experimental and Computational Methods

2.1. Photoelectron Spectroscopy. The experiments were carried out using a magnetic-bottle PES apparatus equipped with a laser vaporization cluster source, details of which have been described previously.[45,46] Briefly, the $B_{11}O^-$ cluster anions were produced by laser vaporization of a pure disk target made of enriched ^{10}B isotope (99.75%) in the presence of a helium carrier gas seeded with 0.01% O_2. The $B_{10}Au^-$ clusters were produced using an Au/B mixed disk target (^{10}B isotope enriched, 99.75%) and a pure helium carrier gas. Cluster anions from the laser vaporization source were analyzed using a time-of-flight mass spectrometer. The $B_{11}O^-$ and $B_{10}Au^-$ clusters of current interest were each mass-selected and decelerated before being photodetached. Two detachment photon energies were used in the current experiments: 266 nm (4.661 eV) and 193 nm (6.424 eV). Effort was made to choose colder clusters (that is, those with long resident times in the nozzle) for photodetachment, which was shown previously to be important for obtaining high quality PES data.[47] Photoelectrons were collected at nearly 100% efficiency by the magnetic bottle and analyzed in a 3.5 m long electron flight tube. The PES spectra were calibrated using the known spectra of Rh^- and Au^-, and the energy resolution of the apparatus was $\Delta E_k/E_k \sim 2.5\%$, that is, ~25 meV for 1 eV electrons.

2.2. Computational Methods. Structural optimizations were carried out at the hybrid B3LYP level,[48] with the augmented Dunning's all-electron basis set (aug-cc-pvtz)[49] for B, O, and H and the Stuttgart relativistic small-core pseudopotential and valence basis set augmented with two f and one g functions [Stuttgart_rsc_1997_ecp + 2f1g: $\alpha(f) = 0.498$, $\alpha(f) = 1.461$, $\alpha(g) = 1.218$] for Au.[50] A variety of initial structures were optimized in search of the ground-state structures of $B_{11}O^-$ and $B_{10}Au^-$ and their neutrals. For the purpose of comparison, the same set of structures was also calculated for $B_{10}H^-$ and $B_{10}H$. Frequency calculations were done to confirm that all obtained ground-state structures are true minima. Excitation energies of the neutrals were calculated with the time-dependent DFT (TDDFT) method[51,52] at the ground-state structures of the anions. All calculations were carried out using Gaussian 03.[53]

3. Experimental Results

3.1. $B_{11}O^-$. The PES spectrum of $B_{11}O^-$ at 193 nm is shown in Figure 1. Its electron binding energies turn out to be rather high. Two well-separated bands (X and A) are revealed between 4 and 5 eV. The ground-state band X is relatively sharp, with a VDE of 4.08 eV (Table 1). Since no vibrational structures are resolved for band X, the ground-state ADE is evaluated by drawing a straight line along the leading edge of band X and then adding the instrumental resolution to the intersection with the binding energy axis. The ground-state ADE for $B_{11}O^-$ so obtained is 4.02 ± 0.04 eV, which represents the electron affinity of neutral $B_{11}O$. Band A (VDE: 4.42 eV) is closely spaced to band X with an excitation energy of less than 0.4 eV. Following a sizable energy gap of ~1 eV, two closely spaced bands B (5.53 eV) and C (5.68 eV) are observed. Another band D is observed at the highest binding energy (VDE: 6.02 eV).

TABLE 1: Observed Adiabatic and Vertical Detachment Energies (in eV) for $B_{11}O^-$ and $B_{10}Au^-$, Compared to the Calculated Binding Energies Based on the C_1 (^1A) Anion Ground-State Structures (1 for $B_{11}O^-$ and 7 for $B_{10}Au^-$) at B3LYP and TDDFT Levels

	feature	ADE (exptl)[a]	VDE (exptl)[a]	channel	VDE (theor)[a,b]
$B_{11}O^-$	X	4.02(4)[c]	4.08(3)	HOMO[d]	3.94
	A		4.42(3)	HOMO−1	4.37
	B		5.53(3)	HOMO−2	5.45
	C		5.68(2)	HOMO−3	5.58
	D		6.02(2)	HOMO−4	5.98
				HOMO−5	6.05
$B_{10}Au^-$	X	3.55(2)[c]	3.64(2)	HOMO[e]	3.50[f]
	A		3.94(2)	HOMO−1	3.81
	B		5.05(5)	HOMO−2	4.93
	C		5.20(5)	HOMO−3	5.09
	D		5.59(2)	HOMO−4	5.61
	E		5.85(3)	HOMO−5	5.65
	F		6.07(2)	HOMO−6	5.94

[a] Numbers in parentheses represent experimental uncertainties in the last digit. [b] The ground-state VDE is calculated at the B3LYP level, whereas those of the excited states are at the TDDFT level. [c] Electron affinity of the neutral species. [d] Computational ADE at the B3LYP level: 3.82 eV. [e] Computational ADE at the B3LYP level: 3.33 eV. [f] The first few VDEs based on the D_{10h} ($^1A_{1g}$) $B_{10}Au^-$ (**11**) are 3.47, 4.46, 6.38, and 6.47 eV.

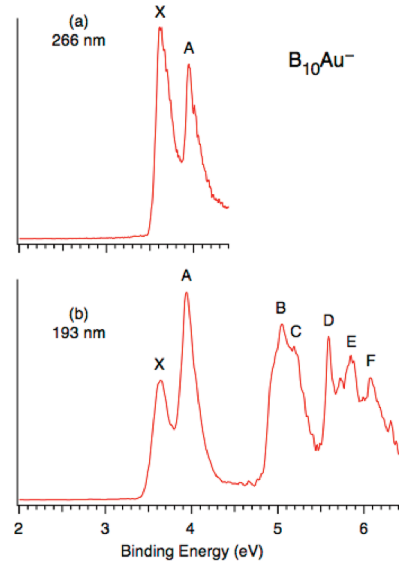

Figure 2. Photoelectron spectra of $B_{10}Au^-$ at (a) 266 nm (4.661 eV) and (b) 193 nm (6.424 eV).

3.2. $B_{10}Au^-$. Figure 2 shows the PES spectra of $B_{10}Au^-$ at 266 and 193 nm. The 266 nm spectrum (Figure 2a) reveals two bands: X (VDE: 3.64 eV) and A (VDE: 3.94 eV). The well-defined onset of band X allows the evaluation of an accurate ground-state ADE for $B_{10}Au^-$ (3.55 ± 0.02 eV), which is also

the electron affinity of $B_{10}Au$ neutral. The relative intensities of bands X and A seem to show photon-energy dependence. Such photon-energy-dependent intensity changes can in principle give valuable information about the nature of the electrons being detached.[54,55] However, in the current case, the detachment channels for the X and A bands are both from delocalized orbitals of the B_{10} ring as will be shown later, and no such information can be extracted from the photon-energy-dependent intensity changes.

The overall PES pattern of $B_{10}Au^-$ at 193 nm (Figure 2b) is surprisingly similar to that of $B_{11}O^-$ (Figure 1), except for a systematic shift to lower binding energies (~0.5 eV; see Table 1). Again, an energy gap (~1.1 eV) is observed between bands A and B. Bands B (5.05 eV) and C (5.20 eV) partially overlap with each other. The higher binding energy portion of the 193 nm spectrum shows numerous features beyond 5.5 eV (Figure 2b), all appearing to be relatively sharp. Three major bands are labeled: D (5.59 eV), E (5.85 eV), and F (6.07 eV).

4. Theoretical Results

Structural searches for the $B_{11}O^-$ and $B_{10}Au^-$ clusters can be demanding computationally. Fortunately, the PES similarities between $B_{11}O^-$ and $B_{10}Au^-$ (Figures 1 and 2) strongly hint that the two species are structurally similar and, therefore, should both possess a B_{10} moiety. Our structural searches are thus largely based on the B_{10} unit, with the extra BO unit and Au attached to different possible sites. Selected optimized structures for $B_{11}O^-$ (**1**−**5**) and $B_{10}Au^-$ (**7**−**12**), along with the ground-state structures of their neutrals (**6** and **13**), are shown in Figure 3.

Briefly, structures **1** (C_1, ^1A), **2** (C_s, $^1A'$), and **3** (C_2, ^1A) of $B_{11}O^-$ can be viewed as the BO unit being attached terminally to three possible peripheral sites of the quasiplanar B_{10}^- cluster[6] in an in-plane fashion. The BO unit prefers a corner site, resulting in anion ground state **1**. Structures **2** and **3** are first-order saddle points, ~40 kcal/mol higher than structure **1**. Structure **5** (C_{2v}, $^1A_1$) can be considered as the BO unit being attached perpendicular to the plane, which is a third-order saddle point, ~86 kcal/mol above structure **1**. Structure **4** (C_{2v}, $^1A_1$) is based on the B_{11}^- moiety[6] with the O atom attached to a peripheral site. It is a second-order saddle point, ~74 kcal/mol above structure **1**. The neutral state **6** (C_1, ^2A) is located as a true minimum, which corresponds to the anion ground state **1**.

Selected structures for $B_{10}Au^-$ (**7**−**12**) and $B_{10}Au$ (**13**) are shown in Figure 3b. Their ground states are **7** (C_1, ^1A) and **13** (C_1, ^2A), respectively. Among these optimized structures, **7**, **9**, **10**, **12**, and **13** correspond to structures **1**, **3**, **4**, **5**, and **6** for $B_{11}O^-/B_{11}O$, respectively. Note that structures **8**, **9**, **10**, and **12** are not minima. Also located for $B_{10}Au^-$ is a highly symmetric wheel structure: **11** (D_{10h}, $^1A_{1g}$), which is a true minimum substantially higher in energy (by 45 kcal/mol). To aid the elucidation of chemical bonding in $B_{11}O^-$ and $B_{10}Au^-$, a similar set of structures are also optimized for $B_{10}H^-$ (**14**−**18**) and $B_{10}H$ (**19**), as shown in Figure 4.

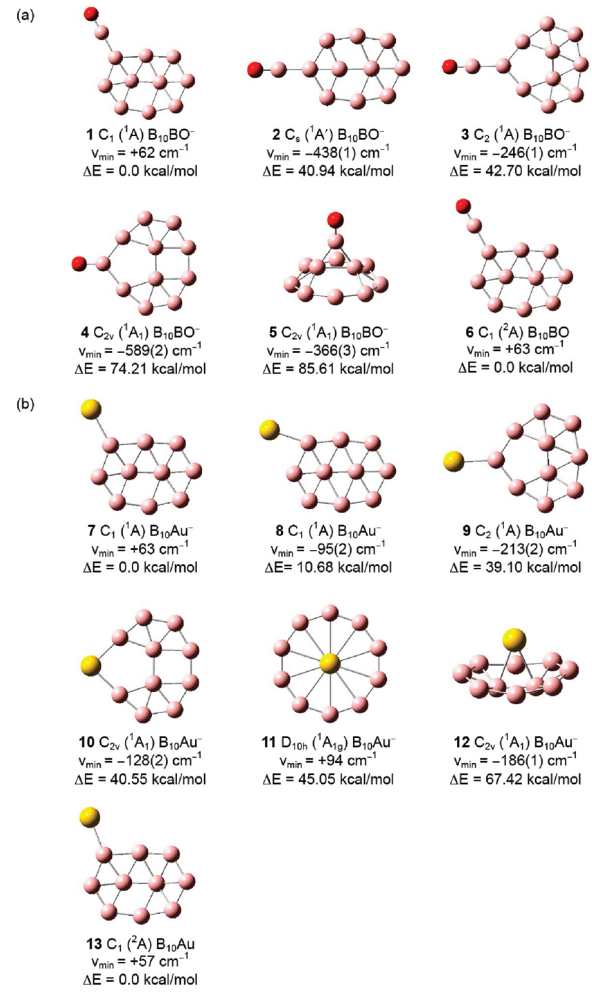

Figure 3. Optimized structures for (a) $B_{11}O^-$ (**1**−**5**) and $B_{11}O$ (**6**) and (b) $B_{10}Au^-$ (**7**−**12**) and $B_{10}Au$ (**13**). The lowest vibrational frequency (ν_{min}) and relative energy (ΔE) are labeled under each structure. The number of imaginary frequencies is shown in parentheses.

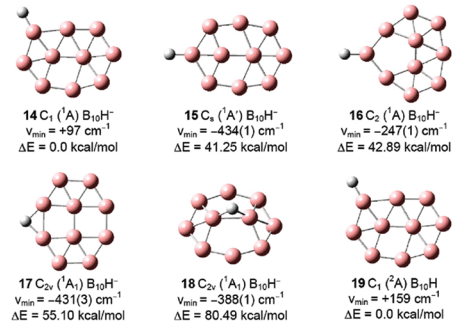

Figure 4. Optimized structures for (a) $B_{10}H^-$ (**14**−**18**) and $B_{10}H$ (**19**). The lowest vibrational frequency (ν_{min}) and relative energy (ΔE) are labeled under each structure. The number of imaginary frequencies is shown in parentheses.

5. Comparison between Experiment and Theory

The well-resolved PES spectra of $B_{11}O^-$ and $B_{10}Au^-$ (Figures 1 and 2) provide electronic and structural information, which helps the search for the global minimum structures through comparison between experiment and theory. As shown in Table 1, the calculated ground-state ADE and VDE for $B_{11}O^-$ (**1**) are 3.82 and 3.94 eV, respectively, as compared to the experimental values of 4.02 and 4.08 eV. For $B_{10}Au^-$ (**7**) the calculated ground-state ADE (3.33 eV) and VDE (3.50 eV) may be compared with the experimental values of 3.55 and 3.64 eV, respectively. It is seen that B3LYP consistently underestimates the ground-state ADE by ~0.2 eV and VDE by ~0.15 eV. For the numerous excited states, TDDFT calculations reproduce the experimental VDE values within ~0.1 eV for the majority of PES bands (Table 1).

The simulated PES spectra for $B_{11}O^-$ and $B_{10}Au^-$ are shown in Figure 5, both in excellent agreement with the experimental data. In particular, the small X−A energy gap and the relatively large A−B energy gap, which are characteristic of the experi-

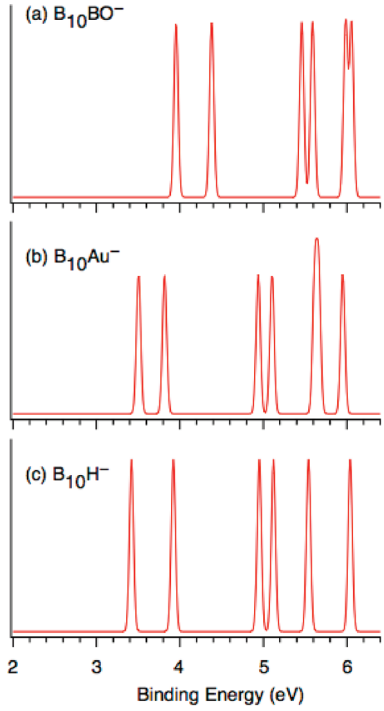

Figure 5. Simulated photoelectron spectra based on the lowest energy C_1 (^{1}A) anion structures for (a) $B_{11}O^-$ (**1**), (b) $B_{10}Au^-$ (**7**), and $B_{10}H^-$ (**14**). The simulated spectra are constructed by fitting the distribution of calculated vertical detachment energy values with unit-area Gaussian functions of 0.05 eV width.

mental PES spectra, are perfectly borne out in the TDDFT calculations. The agreement between experiment and theory is remarkable, lending considerable credence to the identified ground-state structures for both $B_{11}O^-$ and $B_{10}Au^-$ and their neutrals.

6. Discussion

6.1. Structural Similarities between $B_{11}O^-$, $B_{10}Au^-$, and $B_{10}H^-$. The similarity in the PES spectra of $B_{11}O^-$ and $B_{10}Au^-$ is surprising at first glance, suggesting that these two clusters may possess similar structures. The key to the structural connection between $B_{11}O^-$ and $B_{10}Au^-$ is the occurrence of the B_{10} unit and the peripheral BO group in $B_{11}O^-$ (Figure 3a). Both BO and Au can be viewed as monovalent species, which are bonded to the same peripheral site on the B_{10} unit (Figure 3). It is noted that the $B_{11}O^-$ (**1**) ground-state structure, $B_{10}(BO)^-$, differs substantially from that of the bare B_{11}^- cluster,[6] indicating the predominant role of the BO group in governing the structures of boron-rich oxide clusters. The structures of $B_{11}O^-$ and $B_{10}Au^-$ (Figure 3) may be compared to that of $B_{10}H^-$ (Figure 4). The three anion species possess similar global minimum structures (**1**, **7**, and **14**), all involving a B_{10} structural unit, with BO, Au, and H bonded to the same peripheral corner site. The similar structures for $B_{10}X^-$ (X = BO, Au, H) underlie the electronic and structural robustness of the doubly (σ- and π-) aromatic B_{10} cluster as an inorganic building block.[6,8]

6.2. Chemical Bonding in $B_{10}X^-$ (X = H, Au, BO). The B_{10}^- cluster has a C_s (^{2}A″) ground state,[6,56] whose valent molecular orbitals (MOs) are depicted in Figure 6a. The highest occupied molecular orbital (HOMO) is filled by a single electron in the anion. Out of the 15 fully occupied MOs, 9 (HOMO−6 and HOMO−8 through HOMO−15) are responsible for the eight peripheral two-center two-electron (2c−2e) B−B bonds

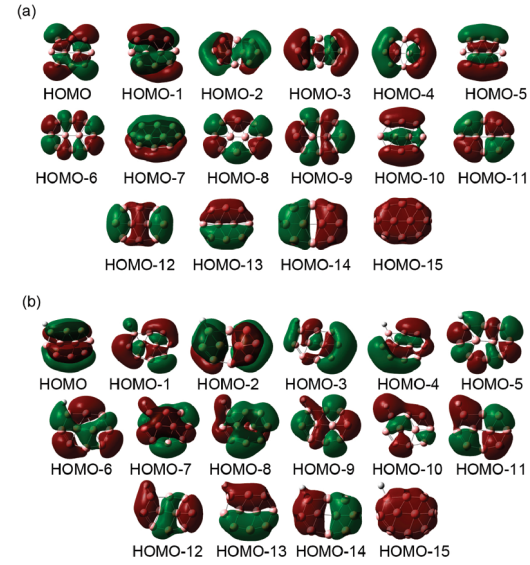

Figure 6. Valence molecular orbital pictures for (a) B_{10}^- and (b) C_1 (^{1}A) $B_{10}H^-$ (**14**).

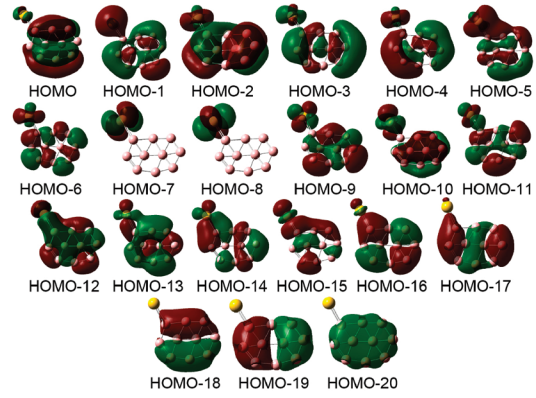

Figure 7. Valence molecular orbital pictures for C_1 (^{1}A) $B_{10}Au^-$ (**7**).

and one 2c−2e bond between the two inner B atoms.[56] The remaining six MOs are responsible for the delocalized global bonding: three MOs (HOMO−1, HOMO−2, and HOMO−7) for the global π-bonding and three MOs (HOMO−3, HOMO−4, and HOMO−5) for the global σ-bonding. Thus the B_{10} neutral possesses double (π- and σ-) aromaticity.

In $B_{10}H^-$ (**14**) the B_{10} moiety retains intact. Except for minor distortions, all 15 fully occupied MOs of B_{10}^- can be found in $B_{10}H^-$ (HOMO through HOMO−9, and HOMO−11 through HOMO−15; Figure 6b), confirming the structural integrity of the B_{10} moiety. The HOMO−10 in $B_{10}H^-$ (Figure 6b) represents the new bonding MO, which may be traced back to the singly occupied HOMO of B_{10}^- (Figure 6a). However, this MO is now composed heavily of the H 1s atomic orbital and primarily represents the B−H single bond.

Compared to $B_{10}H^-$, $B_{10}Au^-$ (**7**) has five more MOs due to the 5d electrons (Figure 7). Despite some mixture with the Au 5d orbitals, the 15 MOs responsible for the bonding in the B_{10} unit can be identified: nine (HOMO−6, HOMO−9, HOMO−11, HOMO−13, and HOMO−16 through HOMO−20) for the localized 2c−2e B−B bonds and one 2c−2e bond between the center B atoms, three MOs (HOMO, HOMO−2, and HOMO−10) for the global π-bonding, and three MOs (HOMO−1, HOMO−3, and HOMO−4) for the global σ-bonding. Five out of six remaining MOs (HOMO−5, HOMO−7, HOMO−8, HOMO−12, and HOMO−14) involve primarily Au 6s/5d atomic orbitals, although B−Au bonding interactions can be

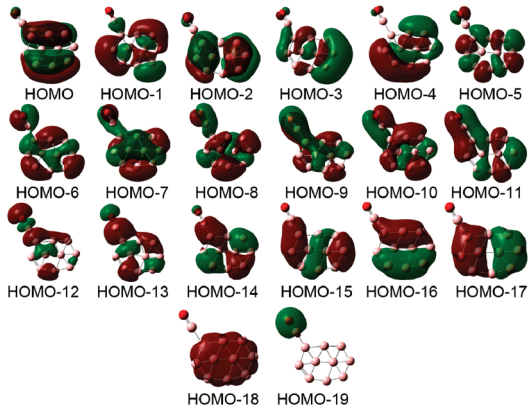

Figure 8. Valence molecular orbital pictures for C_1 (^{1}A) $B_{11}O^-$ (**1**).

seen in HOMO−5, HOMO−12, and HOMO−14. HOMO−15 is the key MO which is responsible for the B−Au σ-bonding. This MO is equivalent to the B−H σ-bonding orbital in $B_{10}H^-$ (**14**, HOMO−10; Figure 6b).

$B_{10}(BO)^-$ (**1**) possesses 40 valence electrons, which occupy 20 MOs as shown in Figure 8. Again, 15 of these MOs can be easily identified for bonding in the B_{10} unit: the localized peripheral 2c−2e B−B bonds and one 2c−2e bond between the two-center B atoms (HOMO−5, HOMO−6, HOMO−8, HOMO−10, HOMO−14 through HOMO−18), delocalized global π-bonding (HOMO, HOMO−2, and HOMO−7), and delocalized global σ-bonding (HOMO−1, HOMO−3, and HOMO−4). Among the remaining MOs, HOMO−9, HOMO−11, and HOMO−12 are responsible for B≡O bonding in the boronyl group, whereas HOMO−19 is the O 2s lone pair. The key bonding MO (HOMO−13) is primarily responsible for the B−BO single σ-bond, which links the B_{10} core and the peripheral BO group. Indeed, HOMO−13 is nearly identical to the corresponding HOMO−10 of $B_{10}H^-$ (Figure 6b) and HOMO−15 of $B_{10}Au^-$ (Figure 7), all of which stem from the σ-bonding interaction between the singly occupied B_{10}^- HOMO and the H, Au, or BO radicals.

Thus, $B_{10}X^-$ (X = H, Au, BO) anions can be considered as covalent complexes between a doubly (σ- and π-) aromatic B_{10}^- core and a monovalent σ-radical, which are linked through a single B−X σ-bond. The calculated B−X bond distances at the B3LYP level are 1.184 Å for $B_{10}H^-$ (**14**), 2.029 Å for $B_{10}Au^-$ (**7**), and 1.628 Å for $B_{10}(BO)^-$ (**1**), which are all typical values for single B−X bonds.[22,35,36] Other than the B−X bond, both B_{10} and X in $B_{10}X^-$ maintain their structural and chemical integrity. For example, the BO group in $B_{10}(BO)^-$ (**1**) retains its triple bond character (HOMO−9, HOMO−11, and HOMO−12; Figure 8), and the B≡O bond distance (1.215 Å at the B3LYP level) matches that of free BO (1.203 Å).[11] As seen from Figures 6−8, the top few occupied MOs (e.g., HOMO through HOMO−4) are similar for $B_{10}(BO)^-$, $B_{10}Au^-$, and $B_{10}H^-$, which underlies the similarity of the PES spectra for $B_{11}O^-$ and $B_{10}Au^-$. The negative charge in the $B_{10}X^-$ anions is located on the B_{10} unit (see the HOMOs of $B_{10}X^-$). Therefore, the B−X covalent bond is similar in the ground states of $B_{10}X^-$ and $B_{10}X$. The B−X bond distances are elongated only very slightly in the neutrals relative to their anions: 0.004 Å for $B_{10}H$, 0.028 Å for $B_{10}Au$, and 0.010 Å for $B_{11}O$.

6.3. On the Viability of the Hypercoordinate D_{10h} $B_{10}Au^-$ Molecular Wheel. The quest of planar hypercoordinate molecular wheels is primarily stimulated by the discovery of pure boron molecular wheels.[5−8] Hypercoordinate molecular wheels containing a boron ring such as D_{6h} CB_6^{2-}, D_{7h} CB_7^-, C_{2v} (effectively D_{8h}) CB_8, D_{9h} AlB_9, and D_{9h} FeB_9^- have been suggested computationally.[37,41−43] However, recent joint experimental and theoretical studies have shown that D_{6h} CB_6^{2-}, D_{7h} CB_7^-, and D_{8h} CB_8 are highly unstable and that carbon avoids the hypercoordinate central position in these species.[38] The highest coordination number in a planar environment observed experimentally to date is eight in the B_9^- molecular wheel.[5] A similar molecular wheel with a nonacoordinate Al has been proposed for AlB_9.[43] There has been interest to design even larger boron rings with a center metal atom, such as the D_{10h} $B_{10}Au^-$.[39]

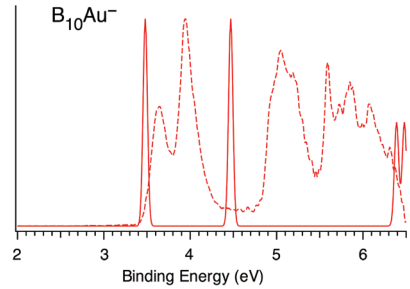

Figure 9. Simulated photoelectron spectrum (solid line) based on the D_{10h} ($^1A_{1g}$) $B_{10}Au^-$ (**11**) anion structure, as compared with the 193 nm experimental data (dashed line). The simulated spectrum is constructed by fitting the distribution of calculated vertical detachment energy values with unit-area Gaussian functions of 0.05 eV width.

Our structural searches indeed find a true D_{10h} ($^1A_{1g}$) minimum for $B_{10}Au^-$ (**11**, Figure 3). However, at the B3LYP level it is 45 kcal/mol above the C_1 (^{1}A) ground state (**7**), and it is not viable experimentally. The simulated PES spectrum based on the D_{10h} $B_{10}Au^-$ anion is shown in Figure 9, where it is compared with the 193 nm experimental PES spectrum. Because of the high symmetry of the D_{10h} isomer, its simulated PES spectrum only contains two peaks in the binding energy regime of 3−6.3 eV. This spectral pattern completely disagrees with the observed PES spectra for $B_{10}Au^-$, confirming the B3LYP result that the D_{10h} isomer is much higher in energy.

Why is the D_{10h} ($^1A_{1g}$) $B_{10}Au^-$ (**11**) minimum so much higher in energy relative to the C_1 (^{1}A) $B_{10}Au^-$ (**7**) ground state? The D_{10h} B_{10} ring is intrinsically electron deficient and would require electron donation from the center atom in the molecular wheel.[39] NBO analyses reveal that the Au center, which has the natural electronic configuration of $6s^{0.45}5d^{9.62}$, carries a positive net atomic charge of q(Au) = +0.90 |e| in D_{10h} $B_{10}Au^-$. However, as a highly electronegative metal, it is energetically not favorable for Au to donate its $6s^1$ valence electron. MO analysis also reveals that the Au center in D_{10h} $B_{10}Au^-$ contributes very little to the "disk delocalization",[5] which would be critical to stabilize the molecular wheel. On the other hand, in the C_1 (^{1}A) $B_{10}Au^-$ (**7**) and C_1 (^{2}A) $B_{10}Au$ (**13**) structures, the integrity and double (σ- and π-) aromaticity of the B_{10} unit are maintained, and the B−Au bonding is primarily covalent: q(Au) = +0.05 and +0.28 |e| in **7** and **13**, respectively. The B−Au covalent bond energy, which is anticipated to be ~3.7 eV,[57] provides additional stabilization to the C_1 ground-state structures. Similar covalent bonding also enhances the stability of the C_1 ground-state structures for $B_{11}O^-$ and $B_{10}H^-$. NBO analysis shows that q(BO) = +0.10 |e|, q(BO) = +0.14 |e|, q(H) = +0.02 |e|, and q(H) = +0.05 |e| for **1**, **6**, **14**, and **19**, respectively. The bonding analyses of the C_1 versus D_{10h} structures of $B_{10}Au^-$ should be valuable for the design of hypercoordinate D_{nh} MB_n molecular wheels.

7. Conclusions

In conclusion, we report a combined photoelectron spectroscopy and density functional theory study on $B_{11}O^-$ and $B_{10}Au^-$

clusters, which give similar PES spectra. DFT calculations show that $B_{11}O^-$ and $B_{10}Au^-$ possess similar C_1 (^1A) structures, which are based on the quasiplanar B_{10} unit with BO and Au bonded to the same peripheral corner site. $B_{11}O^-$ and $B_{10}Au^-$ are thus valent isoelectronic, consistent with their similar PES spectra. The B−BO and B−Au bonding are shown to be highly covalent, analogous to the B−H bonding in $B_{10}H^-$. A highly symmetric D_{10h} ($^1A_{1g}$) molecular wheel is located as a minimum for $B_{10}Au^-$, 45 kcal/mol above the ground state. The current results reinforce the importance of boronyl as a structural unit and the hydrogen analogy of Au, and shed light on the design of D_{nh}-type MB_n molecular wheels.

Acknowledgment. This work was supported by the National Science Foundation (DMR-0904034 to L.-S.W) and the National Natural Science Foundation of China (No. 20873117 to S.-D.L).

References and Notes

(1) Greenwood, N. N.; Earnshaw, A. *Chemistry of the Elements*, 2nd ed.; Butterworth-Heinemann: Oxford, 1997.

(2) Cotton, F. A.; Wilkinson, G.; Murrillo, C. A.; Bochmann, M. *Advanced Inorganic Chemistry*, 6th ed.; John Wiley & Sons: New York, 1999.

(3) (a) Lipscomb, W. N. *Boron Hydrides*; Benjamin: New York, 1963. (b) Lipscomb, W. N. *Science* **1977**, *196*, 1047.

(4) (a) Hanley, L.; Whitten, J. L.; Anderson, S. L. *J. Phys. Chem.* **1988**, *92*, 5803. (b) Kato, H.; Yamashita, K.; Morokuma, K. *Chem. Phys. Lett.* **1992**, *190*, 361. (c) Martin, J. M. L.; Francois, J. P.; Gijbels, R. *Chem. Phys. Lett.* **1992**, *189*, 529. (d) Kawai, R.; Weare, J. H. *Chem. Phys. Lett.* **1992**, *191*, 311. (e) Boustani, I. *Int. J. Quantum Chem.* **1994**, *52*, 1081. (f) Ricca, A.; Bauschlicher, C. W., Jr. *Chem. Phys.* **1996**, *208*, 233. (g) Boustani, I. *Phys. Rev. B* **1997**, *55*, 16426. (h) Gu, F. L.; Yang, X. M.; Tang, A. C.; Jiao, H. J.; Schleyer, P. v. R. *J. Comput. Chem.* **1998**, *19*, 203. (i) Fowler, J. E.; Ugalde, J. M. *J. Phys. Chem. A* **2000**, *104*, 397. (j) Aihara, J. I.; Kanno, H.; Ishida, T. *J. Am. Chem. Soc.* **2005**, *127*, 13324. (k) Oger, E.; Crawford, N. R. M.; Kelting, R.; Weis, P.; Kappes, M. M.; Ahlrichs, R. *Angew. Chem., Int. Ed.* **2007**, *46*, 8503. (l) Szwacki, N. G.; Sadrzadeh, A.; Yakobson, B. I. *Phys. Rev. Lett.* **2007**, *98*, 166804. (m) Tang, H.; Ismail-Beigi, S. *Phys. Rev. Lett.* **2007**, *99*, 115501.

(5) Zhai, H. J.; Alexandrova, A. N.; Birch, K. A.; Boldyrev, A. I.; Wang, L. S. *Angew. Chem., Int. Ed.* **2003**, *42*, 6004.

(6) Zhai, H. J.; Kiran, B.; Li, J.; Wang, L. S. *Nat. Mater.* **2003**, *2*, 827.

(7) (a) Kiran, B.; Bulusu, S.; Zhai, H. J.; Yoo, S.; Zeng, X. C.; Wang, L. S. *Proc. Natl. Acad. Sci. U.S.A.* **2003**, *102*, 961. (b) Sergeeva, A. P; Zubarev, D. Yu.; Zhai, H. J.; Boldyrev, A. I.; Wang, L. S. *J. Am. Chem. Soc.* **2008**, *130*, 7244. (c) Huang, W.; Sergeeva, A. P.; Zhai, H. J.; Averkiev, B. B.; Wang, L. S.; Boldyrev, A. I. *Nat. Chem.* **2010**, *2*, 202.

(8) For a review on all-boron aromatic clusters, see: Alexandrova, A. N.; Boldyrev, A. I.; Zhai, H. J.; Wang, L. S. *Coord. Chem. Rev.* **2006**, *250*, 2811.

(9) Huber, K. P.; Herzberg, G. *Constants of Diatomic Molecules*; Van Nostrand Reinhold: New York, 1979.

(10) Pyykkö, P. *Mol. Phys.* **1989**, *67*, 871.

(11) Zhai, H. J.; Wang, L. M.; Li, S. D.; Wang, L. S. *J. Phys. Chem. A* **2007**, *111*, 1030.

(12) Bauer, S. H. *Chem. Rev.* **1996**, *96*, 1907.

(13) (a) Weltner, W., Jr.; Warn, J. R. W. *J. Chem. Phys.* **1962**, *37*, 292. (b) Sommer, A.; White, D.; Linevsky, M. J.; Mann, D. E. *J. Chem. Phys.* **1963**, *38*, 87. (c) Ruscic, B. M.; Curtiss, L. A.; Berkowitz, J. *J. Chem. Phys.* **1984**, *80*, 3962. (d) Doyle, R. J., Jr. *J. Am. Chem. Soc.* **1988**, *110*, 4120. (e) Hanley, L.; Anderson, S. L. *J. Chem. Phys.* **1988**, *89*, 2848. (f) Burkholder, T. R.; Andrews, L. *J. Chem. Phys.* **1991**, *95*, 8697. (g) Nemukhin, A. V.; Weinhold, F. *J. Chem. Phys.* **1993**, *98*, 1329. (h) Peiris, D.; Lapicki, A.; Anderson, S. L.; Napora, R.; Linder, D.; Page, M. *J. Phys. Chem. A* **1997**, *101*, 9935.

(14) Kawashima, Y.; Endo, Y.; Kawaguchi, K.; Hirota, E. *Chem. Phys. Lett.* **1987**, *135*, 441.

(15) (a) Lory, E. R.; Porter, R. F. *J. Am. Chem. Soc.* **1971**, *93*, 6301. (b) Snelson, A. *High Temp. Sci.* **1972**, *4*, 141. (c) Snelson, A. *High Temp. Sci.* **1972**, *4*, 318. (d) Andrews, L.; Burkholder, T. R. *J. Phys. Chem.* **1991**, *95*, 8554. (e) Lanzisera, D. V.; Andrews, L. *J. Phys. Chem. A* **1997**, *101*, 1482. (f) Bettinger, H. F. *Organometallics* **2007**, *26*, 6263.

(16) Bock, H.; Cederbaum, L.; von Niessen, W.; Paetzold, P.; Rosmus, P.; Solouki, B. *Angew. Chem., Int. Ed. Engl.* **1989**, *28*, 88.

(17) (a) McAnoy, A. M.; Dua, S.; Schroder, D.; Bowie, J. H.; Schwarz, H. *J. Phys. Chem. A* **2003**, *107*, 1181. (b) McAnoy, A. M.; Dua, S.; Schroder, D.; Bowie, J. H.; Schwarz, H. *J. Phys. Chem. A* **2004**, *108*, 2426.

(18) Braunschweig, H.; Radacki, K.; Schneider, A. *Science* **2010**, *328*, 345.

(19) (a) Ehlers, A. W.; Baerends, E. J.; Bickelhaupt, F. M.; Radius, U. *Chem.—Eur. J.* **1998**, *4*, 210. (b) Li, S. D.; Miao, C. Q.; Guo, J. C.; Ren, G. M. *J. Comput. Chem.* **2005**, *26*, 799. (c) Ren, G. M.; Li, S. D.; Miao, C. Q. *J. Mol. Struct.: THEOCHEM* **2006**, *770*, 193. (d) Drummond, M. L.; Meunier, V.; Sumpter, B. G. *J. Phys. Chem. A.* **2007**, *111*, 6539.

(20) Zhou, M.; Jiang, L.; Xu, Q. *Chem.—Eur. J.* **2004**, *10*, 5817.

(21) Zubarev, D. Yu.; Boldyrev, A. I.; Li, J.; Zhai, H. J.; Wang, L. S. *J. Phys. Chem. A* **2007**, *111*, 1648.

(22) Zhai, H. J.; Li, S. D.; Wang, L. S. *J. Am. Chem. Soc.* **2007**, *129*, 9254.

(23) Li, S. D.; Zhai, H. J.; Wang, L. S. *J. Am. Chem. Soc.* **2008**, *130*, 2573.

(24) Yao, W. Z.; Guo, J. C.; Lu, H. G.; Li, S. D. *J. Phys. Chem. A* **2009**, *113*, 2561.

(25) Shao, C. B.; Jin, L.; Fu, L. J.; Ding, Y. H. *Theor. Chem. Acc.* **2009**, *124*, 161.

(26) Ducati, L. C.; Takagi, N.; Frenking, G. *J. Phys. Chem. A* **2009**, *113*, 11693.

(27) (a) Nguyen, M. T.; Matus, M. H.; Ngan, V. T.; Grant, D. J.; Dixon, D. A. *J. Phys. Chem. A* **2009**, *113*, 4895. (b) Tai, T. B.; Nguyen, M. T. *Chem. Phys. Lett.* **2009**, *483*, 35. (c) Tai, T. B.; Nguyen, M. T.; Dixon, D. A. *J. Phys. Chem. A* **2010**, *114*, 2893.

(28) For selected reviews, see: (a) Hall, K. P.; Mingos, D. M. P. *Prog. Inorg. Chem.* **1984**, *32*, 237. (b) Jones, P. G. *Gold Bull.* **1981**, *14*, 102; **1981**, *14*, 159; **1983**, *16*, 114; **1986**, *19*, 46. (c) Whetten, R. L.; Shafigullin, M. N.; Khoury, J. T.; Schaaff, T. G.; Vezmar, I.; Alvarez, M. M.; Wilkinson, A. *Acc. Chem. Res.* **1999**, *32*, 397.

(29) (a) Zhai, H. J.; Bürgel, C.; Bonacic-Koutecky, V.; Wang, L. S. *J. Am. Chem. Soc.* **2008**, *130*, 9156. (b) Wang, X. B.; Wang, Y. L.; Yang, J.; Xing, X. P.; Li, J.; Wang, L. S. *J. Am. Chem. Soc.* **2009**, *131*, 16368.

(30) Wang, L. S. *Phys. Chem. Chem. Phys.* **2010**, *12*, 8694.

(31) Kiran, B.; Li, X.; Zhai, H. J.; Cui, L. F.; Wang, L. S. *Angew. Chem., Int. Ed.* **2004**, *43*, 2125.

(32) Li, X.; Kiran, B.; Wang, L. S. *J. Phys. Chem. A* **2005**, *109*, 4366.

(33) Kiran, B.; Li, X.; Zhai, H. J.; Wang, L. S. *J. Chem. Phys.* **2006**, *125*, 133204.

(34) Zhai, H. J.; Wang, L. S.; Zubarev, D. Yu.; Boldyrev, A. I. *J. Phys. Chem. A* **2006**, *110*, 1689.

(35) Zubarev, D. Yu.; Li, J.; Wang, L. S.; Boldyrev, A. I. *Inorg. Chem.* **2006**, *45*, 5269.

(36) Alexandrova, A. N.; Koyle, E.; Boldyrev, A. I. *J. Mol. Model.* **2006**, *12*, 569.

(37) (a) Exner, K.; Schleyer, P. v. R. *Science* **2000**, *290*, 1937. (b) Wang, Z. X.; Schleyer, P. v. R. *Science* **2001**, *292*, 2465.

(38) (a) Wang, L. M.; Huang, W.; Averkiev, B. B.; Boldyrev, A. I.; Wang, L. S. *Angew. Chem., Int. Ed.* **2007**, *46*, 4550. (b) Averkiev, B. B; Zubarev, D. Yu.; Wang, L. M.; Huang, W.; Wang, L. S.; Boldyrev, A. I. *J. Am. Chem. Soc.* **2008**, *130*, 9248. (c) Averkiev, B. B.; Wang, L. M.; Huang, W.; Wang, L. S.; Boldyrev, A. I. *Phys. Chem. Chem. Phys.* **2009**, *11*, 9840.

(39) Miao, C. Q.; Guo, J. C.; Li, S. D. *Sci. China, Ser. B* **2009**, *52*, 900.

(40) Pu, Z. F.; Ito, K.; Schleyer, P. v. R.; Li, Q. S. *Inorg. Chem.* **2009**, *48*, 10679.

(41) Minyaev, R. M.; Gribanova, T. N.; Starikov, A. G.; Minkin, V. I. *Mendeleev Commun.* **2001**, *11*, 213.

(42) Ito, K.; Pu., Z. F.; Li, Q. S.; Schleyer, P. v. R. *Inorg. Chem.* **2008**, *47*, 10906.

(43) (a) Averkiev, B. B.; Boldyrev, A. I. *Russ. J. Gen. Chem.* **2008**, *78*, 769. (b) Guo, J. C.; Yao, W. Z.; Li, Z.; Li, S. D. *Sci. China, Ser. B* **2009**, *52*, 566.

(44) (a) Erhardt, S.; Frenking, G.; Chen, Z. F.; Schleyer, P. v. R. *Angew. Chem., Int. Ed.* **2005**, *44*, 1078. (b) Islas, R.; Heine, T.; Ito, K.; Schleyer, P. v. R.; Merino, G. *J. Am. Chem. Soc.* **2007**, *129*, 14767. (c) Yang, Z.; Xiong, S. J. *J. Chem. Phys.* **2008**, *128*, 184310. (d) Luo, Q. *Sci. China, Ser. B* **2008**, *51*, 607. (e) Wu, Q. Y.; Tang, Y. P.; Zhang, X. H. *Sci. China, Ser. B, Chem.* **2009**, *52*, 288.

(45) Wang, L. S.; Cheng, H. S.; Fan, J. *J. Chem. Phys.* **1995**, *102*, 9480.

(46) Wang, L. S.; Wu, H. In *Advances in Metal and Semiconductor Clusters*, Vol. 4, Cluster Materials; Duncan, M. A., Ed.; JAI Press: Greenwich, CT, 1998; pp 299−343.

(47) (a) Wang, L. S.; Li, X. In *Clusters and Nanostructure Interfaces*; Jena, P., Khanna, S. N., Rao, B. K., Eds.; World Scientific: River's Edge, NJ, 2000; pp 293−300. (b) Akola, J.; Manninen, M.; Hakkinen, H.; Landman, U.; Li, X.; Wang, L. S. *Phys. Rev. B* **1999**, *60*, R11297. (c) Wang, L. S.; Li, X.; Zhang, H. F. *Chem. Phys.* **2000**, *262*, 53. (d) Zhai, H. J.; Wang, L. S.; Alexandrova, A. N.; Boldyrev, A. I. *J. Chem. Phys.* **2002**, *117*, 7917.

(48) (a) Becke, A. D. *J. Chem. Phys.* **1993**, *98*, 5648. (b) Lee, C.; Yang, W.; Parr, R. G. *Phys. Rev. B* **1988**, *37*, 785.

(49) Kendall, R. A.; Dunning, T. H.; Harrison, R. J. *J. Chem. Phys.* **1992**, *96*, 6796.

(50) (a) Schuchardt, K. L.; Didier, B. T.; Elsethagen, T.; Sun, L.; Gurumoorthi, V.; Chase, J.; Li, J.; Windus, T. L. *J. Chem. Inf. Model.* **2007**, *47*, 1045. (b) Martin, J. M. L.; Sundermann, A. *J. Chem. Phys.* **2001**, *114*, 3408.

(51) (a) Casida, M. E.; Jamorski, C.; Casida, K. C.; Salahub, D. R. *J. Chem. Phys.* **1998**, *108*, 4439. (b) Bauernschmitt, R.; Ahlrichs, R. *Chem. Phys. Lett.* **1996**, *256*, 454.

(52) (a) Li, X.; Kiran, B.; Li, J.; Zhai, H. J.; Wang, L. S. *Angew. Chem., Int. Ed.* **2002**, *41*, 4786. (b) Li, J.; Li, X.; Zhai, H. J.; Wang, L. S. *Science* **2003**, *299*, 864.

(53) Frisch, M. J.; Trucks, G. M.; Schlegel, H. B.; Scuseria, G. E.; Robb, M. A.; Cheeseman, J. R.; Montgomery, J. A.; Vreven, T.; Kudin, K. N.; Burant, J. C.; Millam, J. M.; Iyengar, S. S.; Tomasi, J.; Barone, V.; Mennucci, B.; Cossi, M.; Scalmani, G.; Rega, N.; Petersson, G. A.; Nakatsuji, H.; Kitao, O.; Nakai, H.; Klene, M.; Li, X.; Knox, J. E.; Hratchian, H. P.; Cross, J. B.; Adamo, C.; Jaramillo, J.; Gomperts, R.; Stratmann, R. E.; Yazyev, O.; Austin, A. J.; Cammi, R.; Pomelli, C.; Ochterski, J. W.; Ayala, P. Y.; Morokuma, K.; Voth, G. A.; Salvador, P.; Dannenberg, J. J.; Zakrzewski, V. G.; Dapprich, S.; Daniels, A. D.; Strain, M. C.; Farkas, O.; Malick, D. K.; Rabuck, A. D.; Raghavachari, K.; Foresman, J. B.; Ortiz, J. V.; Cui, Q.; Baboul, A. G.; Clifford, S.; Cioslowski, J.; Stefanov, B. B.; Liu; Liashenko, A.; Piskorz, P.; Komaromi, I.; Martin, R. L.; Fox, D. J.; Keith, T.; Al-Laham, M. A.; Peng, C. Y.; Nanayakkara, A.; Challacombe, M.; Gill, P. M. W.; Johnson, B. G.; Chen, W.; Wang, M. W.; Gonzales, C.; Pople, J. A. *Gaussian 03*, revision A.1; Gaussian, Inc.: Pittsburgh, PA, 2003.

(54) (a) Liu, S. R.; Zhai, H. J.; Wang, L. S. *Phys. Rev. B* **2002**, *65*, 113401. (b) Liu, S. R.; Zhai, H. J.; Wang, L. S. *J. Chem. Phys.* **2002**, *117*, 9758.

(55) Zhai, H. J.; Wang, B.; Huang, X.; Wang, L. S. *J. Phys. Chem. A* **2009**, *113*, 3866.

(56) Zubarev, D. Yu.; Boldyrev, A. I. *J. Comput. Chem.* **2007**, *28*, 251.

(57) (a) Gingerich, K. A. *J. Chem. Phys.* **1971**, *54*, 2646. (b) Barysz, M.; Urban, M. *Adv. Quantum Chem.* **1997**, *28*, 257.

JP108668T